ME-NETT23 The 23rd Conference of the Mechanical Engineering Network of Thailand

DRC

The 23rd Conference of the Mechanical Engineering Network of Thailand
November 4 – 7, 2009, Chiang Mai

Control of Inertial Stabilization Systems Using Robust Inverse Dynamics Control and Sliding Mode Control

Viboon Sangveraphunsiri and Kritsanun Malithong

Department of Mechanical Engineering Chulalongkorn University
254 Phyathai Patumwan Bangkok 10330 Thailand
E-Mail: Viboon.S@eng.chula.ac.th, Kritsanun.M@Student.chula.ac.th, Tel. 0-2218-6449, Fax 0-2218-6583

Abstract

This paper presents an advanced controller strategy for an inertial stabilization system. The system has a 2-DOF gimbal which will be attached to an aviation vehicle. Motion control of gimbal is a difficult task, mainly because of the nonlinearities, dynamics modeling errors, friction and disturbances from the outside environment. A gimbaled stabilization system must stabilize the line of sight toward a target against the external motion induced by aviation vehicle maneuvering and aerodynamic forces. So, an advanced controller is needed. Both robust inverse dynamics control and sliding mode control are implemented in the inner loop or gimbal servo-system to control the gimbal motion. Indirect line of sight (LOS) stabilization will be controlled by the outer loop controller. A stabilizer is mounted on the base of the system to measure base rate and orientation of the gimbal in reference to the fixed reference frame. It can withstand high angular slew rates. The experimental results illustrate that the proposed controllers are capable enough to overcome the disturbances and the impact of LOS disturbances on the tracking performance.

Keywords: Inertial Stabilization / Gimbal / Robust Control / Sliding Mode Control

1. Introduction

At the present, many countries had developed radio control aircraft equipped with video camera and modern surveillance equipment and named “Unmanned Aerial Vehicle” or “UAV”. The initial utilization has been progressing to useful role such as Reconnaissance, Surveillance, Search & Rescue and Telecommunications Relay. A camera gimbal is set up into the aircraft structure. Additionally, the motion of the camera can be controlled remotely from a ground station as well as the airplane.

Motion control can be divided into 2 parts. The first part is controlled by a feedback control system in order to move the gimbal according to a reference command and in the same time to stabilize the gimbal where the camera is attached. Jittter reduction also is needed to be considered in this controller. The second part is the stabilizing of

images done by an image programming technique, which will not be covered in this paper.

There are many works that have been done in this area, such as Li, Hullender and Direnzo [2] purposed a nonlinear induced disturbance rejection, Ambrose, Qu and Johnson [3] purposed a nonlinear robust control for a passive line-of-sight Stabilization system, Li, Hullender [4] purposed a self-turning controller for nonlinear inertial stabilization system. Regional Center of Robotics Technology at Chulalongkorn University has been extending the capabilities of inertial stabilization systems for a number of years. Some Previous capabilities include researching for gimbal structure, gimbal kinematics, gimbal development, and the controller design [8].

This paper focuses on two controllers, the robust inverse dynamics control and the sliding mode control, for stabilizing the servo loop.

2. Gimbal Dynamic Model

The dynamic model of the two-axis gimbal (Fig. 1) can be written in the joint space, by using the Lagrange equation. The friction force, $\mathbf{F}_s$, will be added to the dynamic equations, so the equation of motion in matrix form can be written as:

$$\mathbf{D}(q)\ddot{q} + \mathbf{C}(q,\dot{q})\dot{q} + \mathbf{F}_s \operatorname{sgn}(\dot{q}) + \mathbf{g}(q) = \tau \qquad (1)$$

In this expression, q is the vector of joint angles, τ is the torque vector applied to the joints, $\mathbf{D}(q)$ is the inertia matrix, $\mathbf{C}(q,\dot{q})$ is the vector of centripetal and Coriolis forces, $\mathbf{F}_s$ is an approximated friction forces. $\operatorname{sgn}(\dot{q}) = +1$ when $\dot{q}$ is positive and $\operatorname{sgn}(\dot{q}) = -1$ when $\dot{q}$ is negative. $\mathbf{g}(q)$ is the vector of gravitational forces and function. For this system, each matrix in the dynamic equations can be written as:.

$$\mathbf{D}(q) = \begin{bmatrix} \mathbf{I}_{1_{22}} + \mathbf{I}_{2_{11}} \sin^2\theta_2 + \mathbf{I}_{2_{33}} \cos^2\theta_2 & 0 \\ 0 & \mathbf{I}_{2_{22}} \end{bmatrix}$$

$$\mathbf{C}(q,\dot{q}) = \begin{bmatrix} \frac{1}{2}\omega_2(\mathbf{I}_{2_{11}} - \mathbf{I}_{2_{33}})\times \sin(2\theta_2) & \frac{1}{2}\omega_1(\mathbf{I}_{2_{11}} - \mathbf{I}_{2_{33}})\times \sin(2\theta_2) \\ -\frac{1}{2}\omega_1(\mathbf{I}_{2_{11}} - \mathbf{I}_{2_{33}})\times \sin(2\theta_2) & 0 \end{bmatrix}$$

where $\mathbf{I}_{i_{jk}}$ is a member of row j and column k of moment of inertia of link i.

$$\mathbf{I}_1 = \begin{bmatrix} 0.065 & 0 & 0 \\ 0 & 0.069 & 0 \\ 0 & 0 & 0.07 \end{bmatrix}, \quad \mathbf{I}_2 = \begin{bmatrix} 0.018 & 0 & 0 \\ 0 & 0.024 & 0 \\ 0 & 0 & 0.025 \end{bmatrix}$$

$\mathbf{I}_1$ and $\mathbf{I}_2$ can be obtained by computer aided design software.

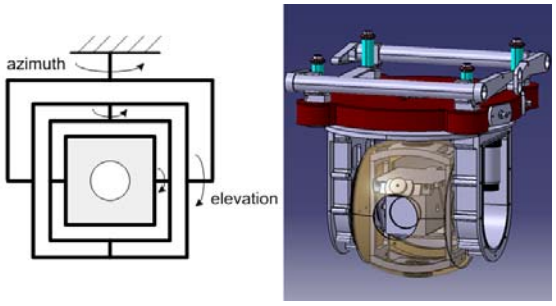

Fig. 1 The two-axis gimbal configuration

3. The Controller Design

Several techniques can be employed for controlling the gimbal motion as well as the way it is implemented. A PID controller is one of the most popular candidates among controllers used for motion control of each motor. For this system, due to disturbances from many sources that affect the motion of the controlled system. More advanced controllers which can stabilize the servo loop more effectively, are need.

The robust inverse dynamics control and the sliding mode control are two candidates for inner loop control or motion control of this system. The indirect stabilization control configuration as shown in Fig. 2 is used to control the overall system, so that the gimbal camera can track the target or maintain its line of sight (LOS). It is called indirect because a stabilizer or rate sensor is mounted on the base of the system to measure the disturbance. The stabilizer

can withstand high angular rates generated during slew and is equipped with a processor to transform the measurement to an equivalent disturbance about the LOS. The motors with controllers are inside the motor block in Fig. 2. The outer-loop controller, with angular rates and orientation information, is for cancellation of the disturbance due to motion of the airplane. A rate sensor is mounted on the base of the gimbal to measure base rate relative to the fixed earth reference frame. The base rate will be transformed to LOS coordinates. The controller will compute commands to reject this disturbance.

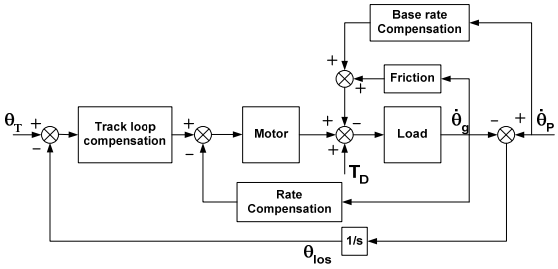

Fig. 2 Indirect LOS Stabilization schematics

In the problem of tracking a joint space trajectory are interested. The system is a nonlinear multivariable system as shown in Eq. (1). The controller technique called nonlinear state feedback can be used to obtain the global linearization of the system dynamics. This is the inverse dynamics control. From the dynamic equation, the control τ can be a function of the system state in the form:

$$\tau = \mathbf{D}(q)y + \mathbf{C}(q,\dot{q})\dot{q} + \mathbf{F}_s \operatorname{sgn}(\dot{q}) + \mathbf{g}(q) \qquad (2)$$

By applying this control, the system Eq. (1) can be described by:

$$\ddot{q} = y \qquad (3)$$

where y can be considered as a new input vector whose expression is to be determined yet. And y can be selected as:

$$y = \ddot{q}_d + K_p(q_d - q) + K_D(\dot{q}_d - \dot{q}) + K_I\int_0^t (q_d - q)dt \quad (4)$$

where $q_d, \dot{q}_d, \ddot{q}_d$ are the desired joint trajectory, joint velocity, and joint acceleration. So, Eq. (3) can be turned into the homogeneous differential equation as:

$$\dddot{\tilde{q}} + K_D\ddot{\tilde{q}} + K_P\dot{\tilde{q}} + K_I\int_o^t \tilde{q}dt = 0 \qquad (5)$$

where $\tilde{q} = q_d - q$. Eq. (5) expresses the dynamics of position error, $\tilde{q}$, while tracking the given trajectory, $q_d, \dot{q}_d, \ddot{q}_d$. The gain K_P, K_D, K_I can be selected by specifying the desired speed of response. From Eq. (2), the control can be computed in real-time based on the parameters of the system dynamic model. In practice, it is difficult to obtain an accurate dynamic model especially in our case. Not only is the model inaccurate, but also the disturbances due to friction and environment change. The robust inverse dynamic and the sliding mode control will be used instead.

3.1 Robust Inverse Dynamics Control

The control vector will be expressed by:

$$\tau = \hat{\mathbf{D}}(q)y + \hat{\mathbf{N}}(q,\dot{q}) \qquad (6)$$

where $\hat{\mathbf{N}}(q,\dot{q})$ is the estimate of:

$$\left(\mathbf{C}(q,\dot{q})\dot{q} + \mathbf{F}_s \operatorname{sgn}(\dot{q}) + \mathbf{g}(q)\right)$$

$\hat{\mathbf{D}}(q)$ is the estimate of $\mathbf{D}(q)$

The control design is based on the assumption that the error of the estimates or the uncertainty is bounded or can be estimated on its range of variation. Even though the uncertainty is unknown, the following assumption is necessary for the control design:

1) Maximum of $\ddot{q}_d$ exists or

$$\sup_{t\geq 0}\|\ddot{q}_d\| \leq Q_m < \infty \quad \text{for all } \ddot{q}_d \qquad (7)$$

2) Bound on Mass Matrix

$$\left\|\mathbf{I} - \mathbf{D}^{-1}(q)\hat{\mathbf{D}}(q)\right\| \leq a \leq 1 \quad \text{for all } q \qquad (8)$$

where $\mathbf{D}(q)$ is positive definite matrix with has upper and lower limited norms. So,

$$d_{\min} \le \left\|\mathbf{D}^{-1}(q)\right\| \le d_{\max} \tag{9}$$

$$\hat{\mathbf{D}} = \frac{2}{d_{\min}+d_{\max}}\mathbf{I} \tag{10}$$

$$\frac{2d_m}{d_{\min}+d_{\max}} \le \left\|\mathbf{D}^{-1}(q)\hat{\mathbf{D}}(q)\right\| \le \frac{2d_{\max}}{d_{\min}+d_{\max}} \tag{11}$$

From Eqs. (8) – (10), it is true that:

$$\left\|\mathbf{D}^{-1}(q)\hat{\mathbf{D}}(q)-\mathbf{I}\right\| \le \frac{d_{\max}-d_{\min}}{d_{\max}+d_{\min}} = a \le 1 \tag{12}$$

3) Bound on Non-linear terms

$$\left\|\hat{\mathbf{N}}(q,\dot{q})-\mathbf{N}(q,\dot{q})\right\| < \infty \text{ for all } q,\dot{q} \tag{13}$$

Substitute Eq. (6) into Eq. (1), we obtain:

$$\mathbf{D}(q)\ddot{q}+\mathbf{N}(q,\dot{q}) = \hat{\mathbf{D}}(q)y+\hat{\mathbf{N}}(q,\dot{q}) \tag{14}$$

Rearrange Eq. (14), we will get:

$$\ddot{q} = y+\left(\mathbf{D}^{-1}(q)\hat{\mathbf{D}}(q)-\mathbf{I}\right)y+\mathbf{D}^{-1}\left(\hat{\mathbf{N}}(q,\dot{q})-\mathbf{N}(q,\dot{q})\right)$$

or

$$\ddot{q} = y-\Gamma \tag{15}$$

where

$$\Gamma = \left(\mathbf{I}-\mathbf{D}^{-1}(q)\hat{\mathbf{D}}(q)\right)y - \mathbf{D}^{-1}\left(\hat{\mathbf{N}}(q,\dot{q})-\mathbf{N}(q,\dot{q})\right) \tag{16}$$

From Eq. (4), let us select the input y is:

$$y = \ddot{q}_d + K_D(\dot{q}_d-\dot{q}) + K_P(q_d-q) + K_I\int_0^t (q_d-q)dt \tag{17}$$

So, Eq. (15) leads to:

$$\dddot{\tilde{q}} + K_D\ddot{\tilde{q}} + K_P\dot{\tilde{q}} + K_I\tilde{q} = \mathbf{N}(q,\dot{q}) \tag{18}$$

Eq. (18) is still non-linear and coupled. It is not guaranteed that the error will converge to zero. Eq. (15) can be rewritten as:

$$\ddot{q}_d-\ddot{q} = \ddot{q}_d-y+\Gamma \rightarrow \ddot{\tilde{q}} = \ddot{q}_d-y+\Gamma \tag{19}$$

Let define state variables as $\eta = \begin{bmatrix}\tilde{q}\\ \dot{\tilde{q}}\end{bmatrix}$

The state equation of Eq. (15) can be written as:

$$\begin{bmatrix}\dot{\eta}\\ \ddot{\eta}\end{bmatrix} = \begin{bmatrix}0 & \mathbf{I}\\ 0 & 0\end{bmatrix}\begin{bmatrix}\eta\\ \dot{\eta}\end{bmatrix} + \begin{bmatrix}0\\ \mathbf{I}\end{bmatrix}(\ddot{q}_d-y+\Gamma) \tag{20}$$

The input y can be selected as usual:

$$y = \ddot{q}_d + K_D\dot{\tilde{q}} + K_P\tilde{q} + K_I\int_0^t \tilde{q}dt + w \tag{21}$$

The term w is to be designed to guarantee robustness to the effects of uncertainty. Substitute Eq. (21) into Eq. (20), we get:

$$\begin{bmatrix}\dot{\eta}\\ \ddot{\eta}\end{bmatrix} = \begin{bmatrix}0 & \mathbf{I}\\ 0 & 0\end{bmatrix}\begin{bmatrix}\eta\\ \dot{\eta}\end{bmatrix} + \begin{bmatrix}0\\ \mathbf{I}\end{bmatrix}\left(-K_D\dot{\tilde{q}}-K_P\tilde{q}-K_I\int_0^t \tilde{q}dt - w + \Gamma\right)$$

$$\begin{bmatrix}\dot{\eta}\\ \ddot{\eta}\\ \dot{\beta}\end{bmatrix} = \begin{bmatrix}0 & \mathbf{I} & 0\\ -K_P & -K_D & -K_I\\ \mathbf{I} & 0 & 0\end{bmatrix}\begin{bmatrix}\eta\\ \dot{\eta}\\ \beta\end{bmatrix} + \begin{bmatrix}0\\ \mathbf{I}\\ 0\end{bmatrix}(\Gamma-w) \tag{22}$$

where $\beta = \int_0^t \tilde{q}dt$. Eq. (22) can be rewritten as:

$$\dot{\zeta} = \mathbf{H}\zeta + \mathbf{G}(\Gamma-w) \tag{23}$$

where $\zeta = \begin{bmatrix}\eta\\ \dot{\eta}\\ \beta\end{bmatrix}$, $\mathbf{H} = \begin{bmatrix}0 & \mathbf{I} & 0\\ -K_P & -K_D & -K_I\\ \mathbf{I} & 0 & 0\end{bmatrix}$, $\mathbf{G} = \begin{bmatrix}0\\ \mathbf{I}\\ 0\end{bmatrix}$

For this system, ζ is a 6×1 vector. The gain K_P, K_D, K_I will be selected so that $\mathbf{H}$ will have eigenvalues with all negative real parts.

Using the Lyapunov direct method to derive the control function w is as follows:

Lyapunov function candidate

$$V = \zeta^T\mathbf{Q}\zeta > 0 \qquad \forall\zeta \tag{24}$$

where $\mathbf{Q}$ is a symmetric positive definite matrix

$$\dot{V} = \dot{\zeta}^T\mathbf{Q}\zeta + \zeta^T\mathbf{Q}\dot{\zeta} \tag{25}$$

$$\dot{V} = \zeta^T\left(\mathbf{H}^T\mathbf{Q}+\mathbf{Q}\mathbf{H}\right)\zeta + 2\zeta^T\mathbf{Q}\mathbf{G}(\Gamma-w) \tag{26}$$

Because $\mathbf{H}$ has negative eigenvalues, so we will have:

$$\left(\mathbf{H}^T\mathbf{Q}+\mathbf{Q}\mathbf{H}\right) = -\mathbf{P} \tag{27}$$

where $\mathbf{P}$ is a symmetric positive definite matrix. So, Eq. (26) becomes:

$$\dot{V} = -\zeta^T\mathbf{P}\zeta + 2\zeta^T\mathbf{Q}\mathbf{G}(\Gamma-w) \tag{28}$$

To make $\dot{V}$ negative definite, we will need $\|w\| \ge \|\Gamma\|$. So, it will be true that:

$$w = \frac{\rho}{\left\|\mathbf{G}^T\mathbf{Q}\zeta\right\|}\left(\mathbf{G}^T\mathbf{Q}\zeta\right), \quad \rho \ge \|\Gamma\| \tag{29a}$$

For small value of $\left\|\mathbf{G}^T\mathbf{Q}\zeta\right\| < \varepsilon$, Eq. (29) will be modified to:

$$w = \frac{\rho}{\varepsilon}\left(\mathbf{G}^T\mathbf{Q}\zeta\right), \qquad \left\|\mathbf{G}^T\mathbf{Q}\zeta\right\| < \varepsilon \tag{29b}$$

The Eq. (29b) is to prevent chattering.

Fig. 3 shows the block diagram of the robust inverse dynamics control. An inertial measurement sensor is added to detect vehicle angular rate and orientation for outer loop control.

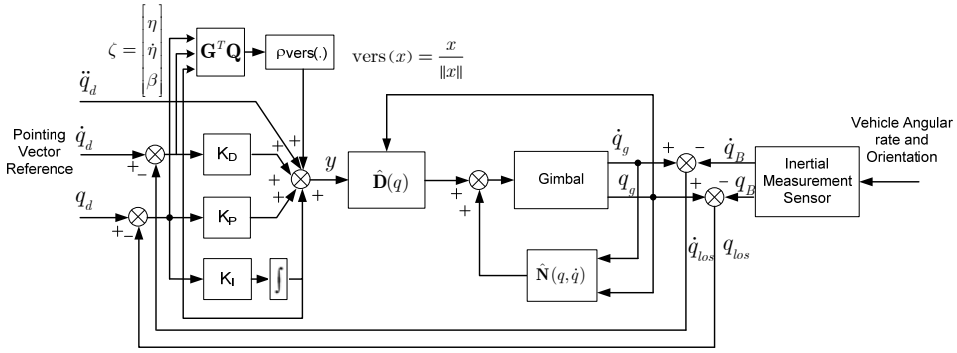

Fig. 3: The block diagram of the robust inverse dynamics control

3.2 Sliding Mode Control

The dynamic equation (Eq. (1)) can be written into state-space description of a non-linear dynamic system as:

$$\dot{x} = f(x) + B(x)u \tag{30}$$

The states are selected as the angular positions and their derivatives

$$x = \begin{bmatrix} x_1 \\ x_2 \end{bmatrix} = \begin{bmatrix} q \\ \dot{q} \end{bmatrix} \tag{31}$$

Then, the following state equations are obtained:

$$\dot{x}_1 = x_2 \tag{32}$$

$$\dot{x}_2 = \ddot{q} = \mathbf{D}^{-1}(x_1)\left[\tau - \mathbf{N}(x_1, x_2)\right] \tag{33}$$

$$= -\mathbf{D}^{-1}(x_1)\mathbf{N}(x_1, x_2) + \mathbf{D}^{-1}(x_1)\tau \tag{34}$$

where $\mathbf{N}(q,\dot{q}) = \mathbf{C}(q,\dot{q})\dot{q} + \mathbf{F}_s\,\mathrm{sgn}(\dot{q}) + \mathbf{g}(q)$

For existence and uniqueness of solution of the above equation, assume that the functions $f(x)$ and $B(x)$ are continuous and sufficiently smooth.

The design of the sliding surface is presented below:

$$\sigma(x,t) = \begin{bmatrix} \sigma_1 \\ \sigma_2 \end{bmatrix} = G_1 e + G_2 \dot{e} = 0. \tag{35}$$

where $e = \begin{bmatrix} e_1 \\ e_2 \end{bmatrix} = \begin{bmatrix} q_{d1} - q_1 \\ q_{d2} - q_2 \end{bmatrix}$ is position error for each joint subsystem, The matrices G_1 and G_2 used in this design are:

$G_1 = \begin{bmatrix} c_{11} & 0 \\ 0 & c_{22} \end{bmatrix}$, $G_2 = \begin{bmatrix} 1 & 0 \\ 0 & 1 \end{bmatrix}$ where c_{11} and c_{22} are positive-definite constants.

The derivation of the control involves the selection of a Lyapunov function $V(\sigma)$ and a desired form for $\dot{V}$, the derivative of the Lyapunov function. The candidated Lyapunov function is:

$$V = \frac{\sigma^T\sigma}{2} \tag{36}$$

For the system given by Eq. (30), and the sliding surface given by Eq. (43), a sufficient condition for the existence of a sliding mode is that:

$$\dot{V} = \sigma^T\dot{\sigma} < 0 \tag{37}$$

The derivative of the Lyapunov function will be negative definite, and this will ensure stability. A stronger condition, guaranteeing an ideal sliding motion, is the η-reachability condition given by:

$$\dot{V} = \sigma^T\dot{\sigma} < -\eta|\sigma| \tag{38}$$

where η is a strictly positive constant.

In a neighborhood of $\sigma = 0$, This is also a condition for reachability. It is desired that:

$$\dot{V} = -\sigma^T K sgn(\sigma). \quad (39)$$

Where K is a positive-definite matrix. Thus, The last two equations together lead to:

$$\sigma^T (K sgn(\sigma) + \dot{\sigma}) = 0 \quad (40)$$

A solution for the equation above is:

$$\dot{\sigma} = -K\,\mathrm{sgn}(\sigma) \quad (41)$$

The expression for the derivative for the sliding function is:

$$\dot{\sigma} = G_1\dot{e} + \ddot{e} \quad (42)$$

$$\dot{\sigma} = G_1\dot{e} + (\ddot{q}_d - \ddot{q}) \quad (43)$$

$$\dot{\sigma} = G_1\dot{e} + \ddot{q}_d - \left(\mathbf{D}^{-1}(x_1)\tau - \mathbf{D}^{-1}(x_1)\mathbf{N}(x_1, x_2)\right) \quad (44)$$

Thus, from Eq. (40) and Eq. (43), we have that:

$$-K sgn(\sigma) = G_1\dot{e} + \ddot{q}_d - \mathbf{D}^{-1}(x_1)\tau + \mathbf{D}^{-1}(x_1)\mathbf{N}(x_1, x_2) \quad (45)$$

$$\tau = \mathbf{D}(x_1)(G_1\dot{e} + \ddot{q}_d) + \mathbf{N}(x_1, x_2) + \mathbf{D}(x_1)K sgn(\sigma) \quad (46)$$

To eliminate the chattering for controller to perform properly, in the sliding mode the signum function in Eq. (46) can be changed by saturation functions as:

$$sat(\sigma_i) = \begin{cases} +1 & if \quad \sigma_i > \Phi_i \\ \dfrac{\sigma_i}{\Phi_i} & if \quad |\sigma_i| \le \Phi_i, \\ -1 & if \quad \sigma_i < -\Phi_i \end{cases} \quad (47)$$

Where $\Phi_i > 0$ is a switching boundary value in joint i.

Fig. 4 shows the block diagram of the sliding mode control. An inertial measurement sensor is added to detect vehicle angular rate and orientation for outer loop control.

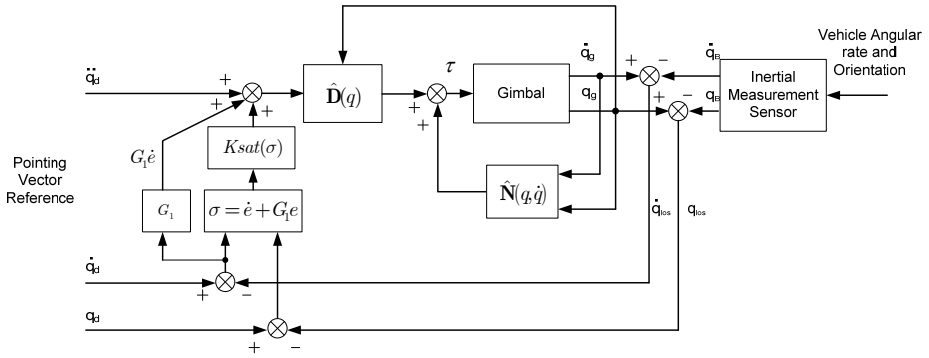

Fig. 4 The block diagram of the sliding mode control

4. Experiment and result

4.1 Experiment method

The experimental setup is shown in Fig. 5. The gimbal is hung freely, so that a base rate disturbance can be generated to emulate close to the real situation. A rate sensor or inertial measurement sensor is mounted on the base of the gimbal to detect the base rate and base orientation reference to the fixed reference frame.

The objective of the control is to maintain LOS position while disturbances and base motion, disturb the system. Robust inverse dynamics control and the sliding mode control are implemented. To test the tracking capability, the reference trajectory $q_d, \dot{q}_d, \ddot{q}_d$ is generated from the trapezoidal velocity profile or s-profile trajectory. The gimbal is swung to generate the slew motion to create the environment motion

close to the real situation. A trapezoidal velocity profile is generated by setting traveling distance, maximum velocity, and maximum acceleration equal to 1 rad, 0.5 rad/sec, and 0.8 rad/sec^2 respectively.

Fig. 5 Experimental and Environment Setup

4.2 Results

The controller must track the input and reject the base rate disturbance at the same time. The disturbance is in the form of shaking the base. The response of azimuth and pitch angle for robust inverse dynamic and sliding mode control are shown in Fig. 6 - 9, respectively. They display the LOS stabilized performance for s-profile trajectory under the disturbance of random signal (Blue line). The experimental results show that the robust inverse dynamics control and the sliding mode control perform very effective for our inertial stabilization system, and are very promising controllers.

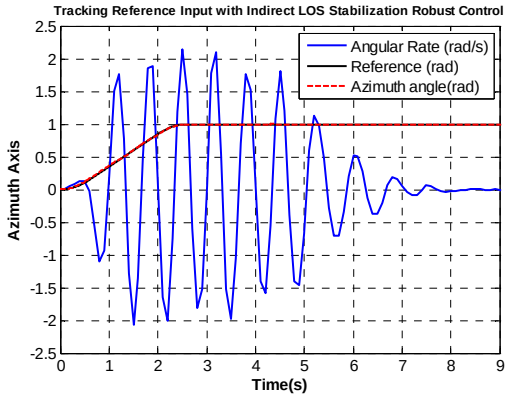

Fig. 6 The response of azimuth axis, using the robust inverse dynamics control.

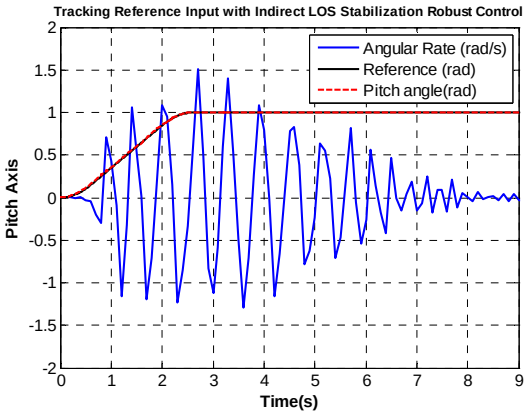

Fig. 7 The response of pitch axis, using the robust inverse dynamics control.

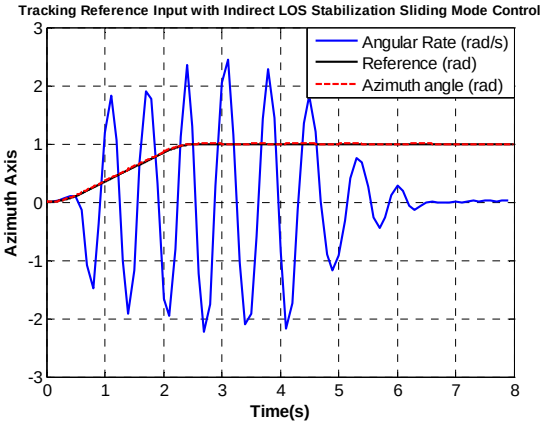

Fig. 8 The response of azimuth axis, using the sliding mode control.

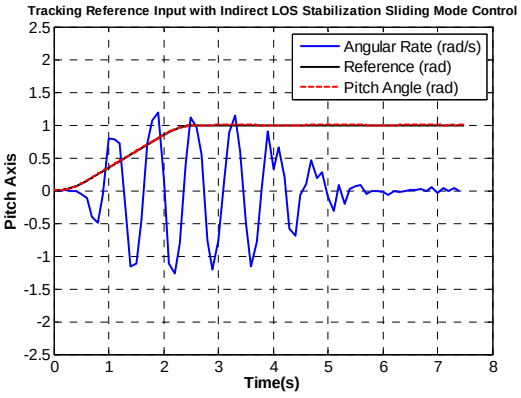

Fig. 9 The response of pitch axis, using the sliding mode control.

5. Conclusion

The details of the two controllers, the robust inverse dynamic and the sliding mode control, of a two-axes gimbal configuration are

described. The experiment results in a two-axes gimbal are presented to verify the effectiveness of the proposed method in rejecting carrier disturbances. The robust inverse dynamic and the sliding mode control can be used for low-level motion control of the gimbal. Indirect stabilization is for reducing the jittering due to base rate disturbances. Unbalanced mass and friction can also be compensated by integral action.

6. References

[1] Kenady, P. J. (2003). Direct Versus Indirect Line of Sight (LOS) Stabilization, IEEE Transactions on control systems technology, Vol. 11, No.1, January 2003

[2] Li, B., Hullender, D. and DiRenzo M. (1998). Nonlinear Induced Disturbance Rejection in Inertial Stabilization Systems, IEEE Transactions on control systems technology, Vol. 6, No.3, May 1998

[3] Ambrose, H., Qu, Z., Johnson, R. (2001). Nonlinear Robust Control For A Passive Line-of-Sight Stabilization System, Proceedings of the 2001 IEEE International Conference on Control Applications, September 5-7, 2001, Mexico

[4] Li, B. and Hullender, D (1998). Self-Tuning Controller for Nonlinear Inertial Stabilization System, IEEE Transactions on control systems technology, Vol. 6, No.3, May 1998.

[5] Becker, G., Cubalchini, R., Tham, Q. and Anagnost, J. (1999). Generation of Structural Design Constraints for Spaceborne Precision Pointing System, Proceedings of the 2001 IEEE International Conference on Control Applications, Hawaii, USA, August 1999.

[6] Yoon, S. and Lundberg, J. B. (2001). Equations of Motion for a Two-Axes Gimbal System, IEEE Transactions on Aerospace and Electronic system, Vol. 37, No.3, July 2001.

[7] Gosselin, C. M and Hamel, J.F. (1994). The agile eye: a high-performance three-degree-of-freedom camera-orienting device, 1994, Proceedings of the IEEE.

[8] Wongkamchang, P., Sangveraphunsiri, V. (2008). Control of Inertial Stabilization Systems Using Robust Inverse Dynamics Control and Adaptive Control. The Thammasat International Journal of Science and Technology, 2008, Volume 13, No. 2, pp. 20 – 32.

[9] Craig, J.J. (1989). Introduction to Robotics mechanics and control, 2nd edition, Silma, Inc.

[10] Slotine, J.-J.E. (1987). Robust Control of Robot Manipulators, Int. J. Robotics Research.

[11] Edward, C., Spurgeon, S.K. (1998) Sliding Mode Control: Theory and Applications, T.J. International Ltd, Padstow, UK

[12] Slotine, J.-J.E., Li, W., (1991). Applied Nonlinear Control, ISBN 0-13-040049-1, Prentice -Hall International, Inc., New Jersey.